Timeresolved stimulated Raman scattering in a diamond anvil cell

Michael Baggen, Martin van Exter, and Ad Lagendijk

Time-resolved stimulated Raman scattering in a diamond anvil cell

Michael Baggen, Martin van Exter, and Ad Lagendijk

*Natuurkundig Laboratorium der Universiteit van Amsterdam, Valckenierstraat 65, 1018 XE Amsterdam,
The Netherlands*

We demonstrate the first application of picosecond stimulated Raman scattering in a diamond anvil cell. A study of vibrational relaxation as a function of pressure is made. As a model system, we choose the totally symmetric C–C stretching mode of benzene and benzene-d_6. Measurements of the transverse relaxation time have been performed at room temperature in the pressure range up to 5 GPa. A pronounced difference in the pressure dependence of the relaxation time is observed between the fluid phase, solid phase I, and solid phase II. We also observed another interesting phenomenon: the ratio of the isotropic Raman and nonresonant contribution to the nonlinear susceptibility appears to increase with pressure.

I. INTRODUCTION

In the past decade, the study of vibrational relaxation (VR) in molecular condensed phases has received considerable interest. The relaxation processes can be separated in energy and phase relaxation mechanisms. In analogy with NMR spectroscopy they are termed T_1 and T_2 processes. The traditional spectroscopic tool for studying these processes is spontaneous Raman scattering (SpRS). Measurements of the isotropic and anisotropic Raman spectra make it possible to distinguish between reorientational and vibrational relaxation processes.

High pressure plays an important role in the study of molecular condensed phases. In general, these substances are very compressible, so even at modest pressures, the density, and therefore, the intermolecular distance, can be varied over a large range. For this reason the combination of Raman spectroscopy and high-pressure techniques, especially the diamond anvil cell (DAC), has become a valuable tool in studying the dynamics of molecular condensed phases.[1]

In more recent years, the use of time-resolved nonlinear optical techniques provides the means of probing relaxation phenomena in the time domain.[2] In this paper, we will deal with the technique called time-resolved stimulated Raman scattering (TSRS). Recently it was shown[3] that TSRS produces information about the magnitude and phase of the third-order susceptibility $\chi^{(3)}$. Apart from vibrational and reorientational dynamics a nonresonant contribution is measured. The relationship between TSRS and SpRS is a simple one for strongly polarized Raman lines. For a homogeneous broadened line of Lorentzian shape, the relaxation time T_2 is the reciprocal of the linewidth $\Delta \nu_{1/2}$:

$$T_2 = (2\pi c \Delta \nu_{1/2})^{-1}. \tag{1}$$

A combination of time-resolved spectroscopy and high pressure range would offer a unique access to studying the mechanisms of VR. To show the feasibility of such an experiment, we decided to study the relaxation of the totally symmetric (a_{1g}) C–C stretching modes of C_6H_6 and C_6D_6.

The phase diagram of benzene has been studied by several authors and shows a number of transitions.[4-6] Under atmospheric pressure conditions, the liquid state exists down to 279 K. It crystallizes in the solid phase I, that has an orthorhombic structure with four molecules per unit cell. This phase is observed to exist at least down to 1.6 K. At room temperature (295 K) benzene solidifies at a pressure of 60 MPa, also forming phase I. At about 1.4 GPa, a pressure induced phase transformation into the monoclinic phase II takes place. Increasing the pressure still further will result in the formation of phase III (4 GPa) and phase IV (9 GPa), both of yet unknown structure. However, they fall beyond the pressure range of our study.

Benzene and benzene-d_6 have served as a model system for the study of VR, especially in the liquid state. Griffiths *et al.*[7] showed that the linewidth of the C–C mode in pure liquid benzene and benzene-d_6 is 2.1 and 1.5 cm^{-1}. Following Eq. (1), this corresponds to a relaxation time of 5.0 and 7.1 ps, respectively. They pointed out that this is a large difference for the same mode in essentially equivalent molecules. In a dilution experiment, they demonstrated the presence of (near) resonant energy transfer in benzene, accounting for 33% of the linewidth. In benzene-d_6, this contribution to the total linewidth seems less pronounced.

Tanabe and Jonas[8] measured the Raman linewidth of several internal modes of liquid benzene-d_6 in the pressure range extending up to the melting pressure between 303 and 393 K. The linewidth of the 945 cm^{-1} mode shows an increase both with pressure and temperature. A VR model based on pure dephasing mechanisms[9] is used to describe the observed behavior. Data quoted by Tanabe and Jonas from the Ph.D. thesis of Campbell[10] showed similar results for benzene.

Data on VR in crystalline benzene are mainly available in the low temperature regime (notably 1.6 K) from a series of CARS studies by Trout *et al.*[11] and Ho *et al.*[12] At these temperatures, relaxation is dominated by T_1 processes, leading to a decay time of 50 ps for isotopically pure benzene.

In the rest of this paper we will discuss some theoretical aspects of TSRS and give a description of the experiment. Attention will be paid to the choice of the focusing geometry.

The data of the high pressure TSRS and SpRS measurements will be presented, together with the discussion of the results and possible applications of this method to other systems.

II. THEORY OF TSRS

TSRS, first proposed by Heritage,[13] employs two parallel-pumped tunable cw mode-locked dye lasers of different frequency (ω_l, ω_s), whose frequency difference Ω is tuned to the internal mode of the system. One synchronized pulse pair is used to create (pump) a coherent excitation of the mode; a second pair, after a variable delay, probes the relaxation of the mode coherence. As the delay is scanned, one observes rapid oscillations (gain, loss) in the energy transfer ΔI_s to the lower frequency beam ω_s. These oscillations correspond to the Raman frequency, with an envelope that represents the decay of the coherent excitation.

The increase in power ΔI_s of the probe beam is given by[2]

$$\Delta I_s = \text{Re}\left[\frac{1}{4} i\omega_s L e^{i\Omega\Delta} \int_{-\infty}^{\infty} C(\Delta - \tau)d(\tau)e^{-i\Omega\tau}d\tau \right], \tag{2}$$

where L is the length of the sample, Δ is the time delay between the pump and the probe pair,

$$C(t) = \int_{-\infty}^{\infty} E_l(x)E_s^*(x)E_l^*(x+t)E_s(x+t)dx \tag{3}$$

is a higher-order correlation function (FWHM $= \gamma_c$) of the electric laser fields

$$\mathbf{E}(\mathbf{r},t) = 1/2\mathbf{e}_x\{E_s(z,t)e^{-i(\omega_s t - k_s z)}$$

$$+ E_l(z,t)e^{-i(\omega_l t - k_l z)} + \text{c.c.}\}, \tag{4}$$

and $d(\tau)$ is the response function of the system under investigation. Assuming exponential decay of the excitation, the following model for $d(t)$ can be obtained:

$$d(t) = -iA\, e^{-t/T_2} e^{i\omega_0 t}\theta(t) + 3/2\sigma\delta(t), \tag{5}$$

where T_2 is the relaxation time of the Raman mode, ω_0 is its eigenfrequency, and $\theta(t)$ is the step function. The quantity A measures the nuclear contribution and represents the isotropic part of the Raman excitation (the anisotropic contribution B can be included in a similar way). The nonresonant contribution is represented by σ; the decay of this contribution is usually very fast, so the response to the driving field $C(t)$ is considered to be instantaneous.

We shall investigate four cases which are of particular relevance for a TSRS experiment:

(1) $(\Omega = \omega_0$, scan of $\Delta)$. The mode is driven on resonance, and its time evolution is described by Eq. (5). In the case of an exponential decay, the relaxation time T_2 corresponds to the slope of the curve, plotted on a logarithmic scale.

(2) $(\Omega \neq \omega_0$, scan of $\Delta)$. The response contains only the nonresonant part σ. In this way the driving field $C(t)$ is obtained.

(3) (scan of Ω, $\Delta = 0$). A scan of the frequency Ω contains both the Raman (A) and nonresonant (σ) contribution convoluted with the driving field $C(t)$.

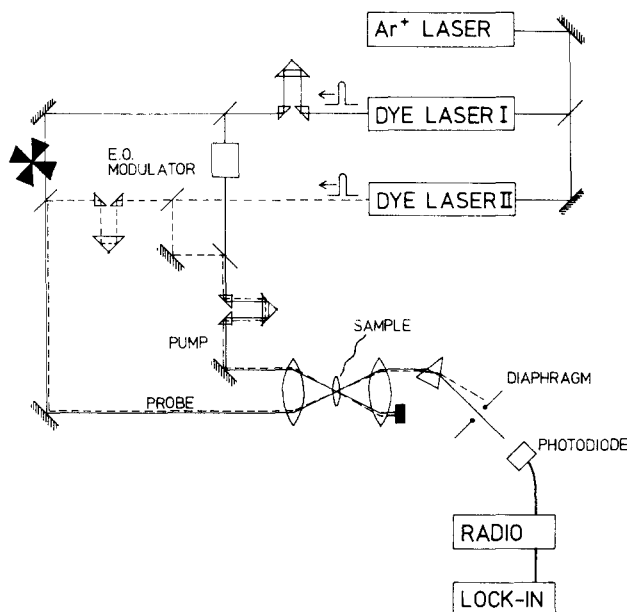(4) (scan of Ω, $\Delta > 0$). This frequency scan contains

FIG. 1. The laser system used to generate the TSRS signal. For explanation see the text.

only resonant contributions. The response reaches its maximum value when Ω is equal to the eigenfrequency of the mode ω_0. Experimentally, this is a good way to tune the Raman mode and obtain a reading of the oscillator strength A.

III. EXPERIMENTAL

The laser system used to generate the TSRS signal is shown in Fig. 1. It consists of two dye lasers (Spectra Physics 375 + 375B), synchronously pumped by a mode-locked Ar^+ laser (Spectra Physics 171). Rhodamine 6G is used as a dye medium. The delay of the probe pair with respect to the pump pair is obtained using a home-built delay table. The detection of the induced gain/loss of the probe beam is performed with a double modulation technique and an AM radio,[14] resulting in a detectable gain limit of 10^{-7}. The data, together with the position of the delay line, are digitized and stored on an IBM PC, equipped with a Tecmar Labmaster interface board.

Benzene and benzene-d_6 are both obtained from Merck (Uvasol: purity $> 99.7\%$). No further purification is performed. The DAC used in this experiment is described by Silvera and Wijngaarden.[15] The pressure in the sample is determined with the well-known ruby fluorescence technique.

Apart from the time-resolved measurements we recorded ordinary SpRS spectra of the 992 cm^{-1} mode under pressure, as well as the lattice modes (for pressures higher than 3 GPa). The spectra were taken in backscattering on a Spex 1402 double monochromator equipped with a cooled Hamamatsu phototube (model R943-02). The data from the SSR photo-counting unit are digitized and transferred to an IBM PC that also controls the stepper motor of the Spex.

The prime challenge performing TSRS in a DAC is the choice of the focusing geometry. The energy transfer to (from) the probe beam takes place in the focal overlap of the
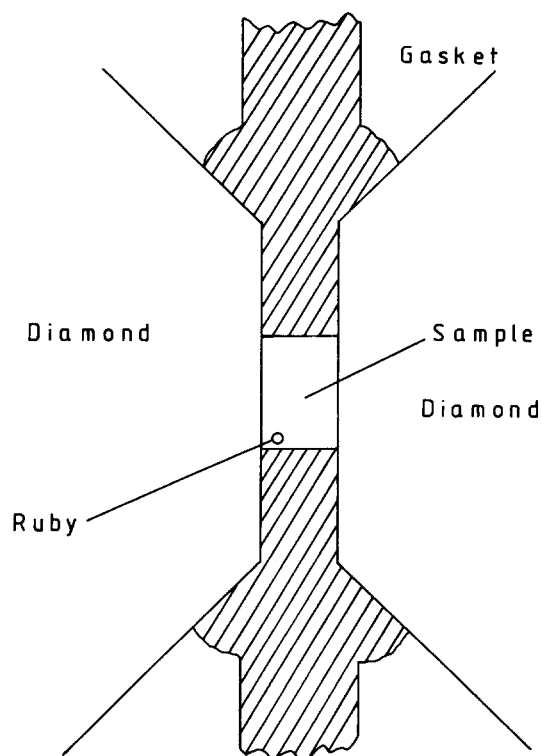
FIG. 2. Closeup of the DAC gasket, sample hole, and diamonds. The diameter and initial thickness of the sample hole is 0.2 mm. The diamond culet is 0.6 mm. The ruby chip is loaded with the sample for pressure calibration. The gasket material is T 301 stainless steel.

pump and probe beams. In experiments with bulk samples, both beams (diameter 1 mm) are focused in the sample with one lens. In order to separate the pump from the probe, they cross each other in the sample at a small angle. In this case, the TSRS signal is not extremely sensitive to the lens quality or the focal length of the spots. The stimulated Raman gain at zero delay is in the order of 10^{-4}, with a peak power of 15 W incident on the sample.

The situation changes when the sample is placed in the gasket hole of the DAC. A close-up of the gasket and diamonds is given in Fig. 2. The sample chamber is a cylindrical hole created by spark erosion in a stainless steel gasket (T301). Its initial length and diameter are 0.2 mm; these values will decrease upon compression. The two diamonds have a thickness of 2 mm each. In this geometry, the focal overlap region may contain the benzene sample, but also a part of the surrounding diamonds. This results in a TSRS signal with contributions from both materials. However, in contrast to the diamonds, the benzene mode is probed on resonance. Thus the diamond contribution consists of the (unwanted) nonresonant part of $\chi^{(3)}$.

In order to reduce this contribution, the length of the focal overlap region has to be minimized. Taking into account the refractive index of the sample ($n = 1.5$), this implies a focal length (in air) of 135 μm. A focal length of this magnitude cannot be achieved by using a single microscope objective, because the design of the DAC sets a lower limit to the working distance of the lens of 35 mm. So we decided to use a double lens system. The first lens (planoconvex

$f =$ 120 mm) magnifies the original beam diameter of 1 mm by a factor of 6.4. The second lens (a Wild Heerbrugg microscope objective $f =$ 75 mm) focuses each beam in a spot of 170 μm depth and a width of 5 μm, corresponding to a peak-power density of 0.1 GW cm^{-2} in the benzene sample, and much lower in the surrounding diamonds. This power density implies that nonlinear effects like self-focusing are not important in this experiment. The magnification of the beams is limited by the acceptance angle of the DAC (30°). Due to the large magnification, the total aperture of the second lens is used. This requires a lens of low spherical distortion.

The lens combination described above is one composed from a series of ten combinations we tried. The final criterion for spherical aberration is given by the signal ratio of the two lens to the single lens geometry when working with a bulk sample. The combination employed by us yielded a ratio of 82%. The effect of the focal length was estimated from the ratio of the two-lens DAC signal and the two-lens bulk signal; a characteristic value for this parameter is 60%. An estimate for the focal length can be given by measuring the TSRS signal as a function of the position of the DAC with respect to the focusing lens: A length of 120 μm between the 1/e points is found, in qualitative agreement with the calculated focal length.

IV. RESULTS

In this section we will report on the TSRS and SpRS data of the benzene and benzene-d_6 C–C modes under pressure. Following the procedures outlined in the theory section, the form of $C(t)$ was obtained. It can be approximated by a power of cosh $(t/1.9)$ with t in picoseconds. The power τ varies between 1.3 and 2.1. This corresponds to a FWHM γ_c of 3.5 to 3.0 ps, depending on the setting of the dye lasers. The features of $C(t)$ are Gaussian in the top and exponential in the wings.
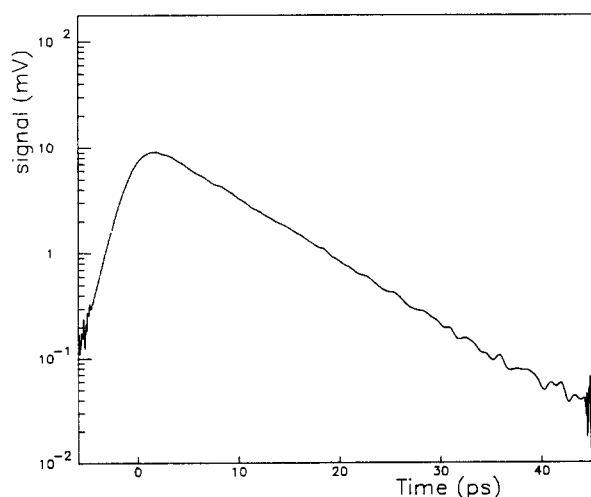

FIG. 3. Typical time-resolved stimulated Raman scan of a benzene sample in the DAC at a pressure of 1.55 GPa after digital filtering. The rapid oscillations corresponding to the Raman frequency are not shown here. The decay of the mode coherence is exponential and can be traced over two decades. The relaxation time in this case is 7.5 ps.
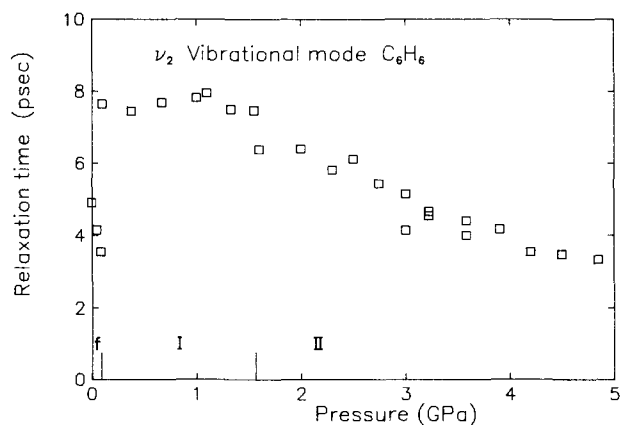
FIG. 4. Experimental data for the transverse relaxation time vs pressure for benzene. The fluid (f) and solid phases I and II are indicated.

FIG. 6. Experimental data for transverse relaxation time vs molar volume for benzene, using the EOS from Refs. 16 and 17.

Figure 3 represents a typical time-resolved run of the benzene ν_2 mode in the DAC after processing and digital filtering of the data. Only the envelope corresponding to the decay of the coherent excitation is shown here, without the underlying Raman oscillations. The decay is exponential, indicating a Lorentzian line shape, and can be traced over 2.5 decades. This should be compared to 5 decades in a CARS experiment. The accuracy of T_2 is typically 0.2 ps. At higher pressures, the transparency of the sample decreases, resulting in beam distortion and a lower signal to noise ratio.

The pressure dependence of the relaxation time T_2 of this mode is plotted in Figs. 4 (benzene) and 5 (benzene-d_6). The liquid state shows a strong decrease of relaxation time, upon increase of the pressure from zero to the melting line. Benzene shows a drop from 4.9 to 3.5 ps, and benzene-d_6 a corresponding drop from 6.9 to 4.7 ps. The zero pressure values are in good comparison with the data by Griffiths et al.[7] quoted in Sec. I. The linewidth decrease observed by Tanabe and Jonas[8] for C_6D_6 however shows a weaker pressure dependence than the one observed in this work. At crystallization into phase I, a remarkable increase is observed by a factor 2.1 (benzene) and 1.7 (benzene-d_6): at higher pressures, it starts to decrease again. For normal deuterium, a
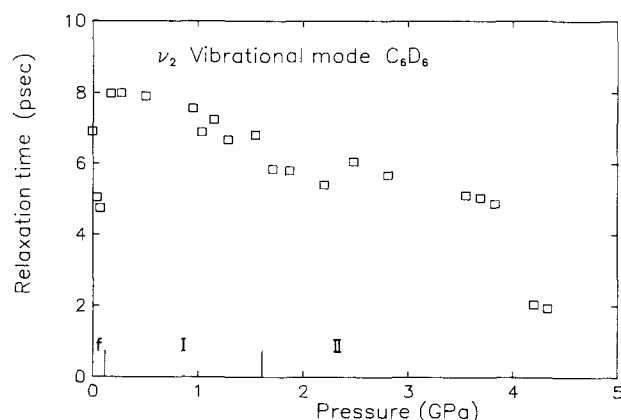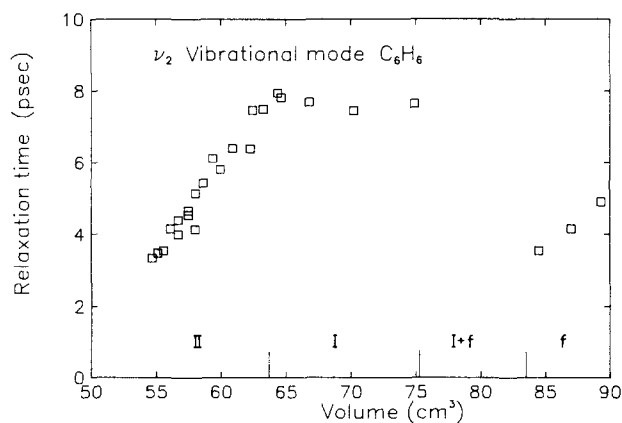
Raman linewidth study by Sharma et al.[18] in the pressure range up to 50 GPa (300 K) reveals a similar decrease of the relaxation time in the liquid state and a sharp increase (by a factor of 1.7) on solidification. Using the benzene equation of state data by Bridgman[16] and Figuiere,[17] the relaxation time as a function of molar volume is given in Fig. 6. Note that T_2 shows a (quasi) linear dependence of the molar volume in the liquid and solid phase II range.

The mode frequency ω_0 is also a function of pressure. Figure 7 shows data for C_6H_6 obtained from TSRS as well as SpRS measurements. Starting at 992 cm^{-1} in the liquid phase, it increases linear with pressure up to 1.5 GPa. At higher pressures, the line splits into two components: the lower component is attributed to the solid phase I, whereas the higher one belongs to phase II. Factor-group splitting in these phases is much smaller and does not interfere, due to the fact that $\chi^{(3)}_{1111}$ contains only the a_{1g} mode.[11] The presence of this line splitting became manifest when we observed beat patterns in the time-resolved runs, the beat frequency corresponding to the magnitude of the splitting (5.0 cm^{-1} at 2.75 GPa). By tuning Ω to each of the two components, their relaxation rate could be probed separately. After annealing

FIG. 5. Experimental data for the transverse relaxation time vs pressure for benzene-d_6.
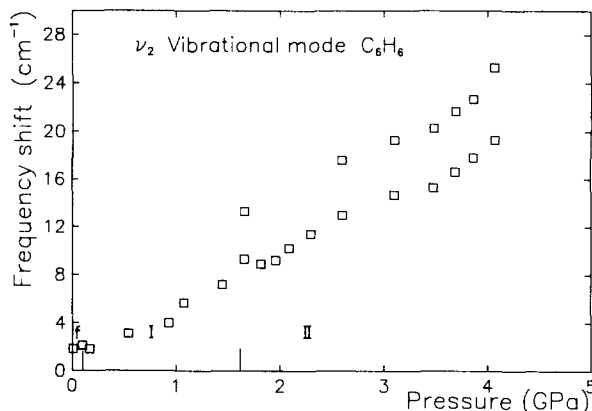

FIG. 7. Experimental data for the frequency shift of the benzene C–C stretching mode vs pressure. Zero frequency shift corresponds to 992 cm^{-1}. An unannealed sample was used. For pressures higher than 1.5 GPa, two lines are observed: the lower mode corresponding to the metastable phase I, the higher one to phase II.

of the sample, the lower frequency component has almost vanished, indicating the transformation of phase I into phase II. The sluggish character of the phase transformation has been observed by several other authors.[4–6] The splitting in C_6D_6 behaved in a similar way.

The ratio of nonresonant and Raman contributions for the benzene mode yields a value for A/σ of 0.7 ps^{-1} in the liquid state. On solidification, this changes to 1.8 ps^{-1}, and a gradual increase with pressure is observed (0.3 ps^{-1}/GPa). However, there is always a nonresonant contribution due to the diamonds, which we estimate to be 40% at low pressures (1.55 GPa). Due to deformation of the gasket, this may become even larger at higher pressures.

V. DISCUSSION

Several models have been developed to explain the pressure dependence of the relaxation rate in the liquid phase, e.g., the dephasing model by Fisher and Laubereau.[17] The model is based on the isolated binary collision (IBC) approximation, separating the time scale on which the interaction takes place and the interval between collisions. This model is used by Tanabe and Jonas[7] to describe the essential features of the linewidth behavior in benzene-d_6. On solidification however, the concept of IBC seems to loose its validity. One line of approach here would be to decompose local displacements into elementary excitations (phonons, librons, and vibrons). This is most useful at very low temperatures since an expansion can be made in the number of elementary excitations involved in the dephasing process. At high temperatures this seems a difficult road to follow.

The need for a better theoretical understanding of dephasing mechanisms is very prominent. In many of the current approaches a weak-coupling formalism is used. In this case the most important ingredient in the expressions for the dephasing time are bath correlation functions, e.g., velocity–velocity correlation functions. Probably the most reliable method of calculating these correlation functions is the molecular dynamics (MD) computer simulation technique. In our experimental work the density is varied over a substantial range (a factor of 2) and it includes the liquid–solid transition, all at the same temperature. This forms a serious test for the theory. In a recent article by Chesnoy and Weis[19] a MD simulation is used to calculate the density dependence of the bath correlation functions relevant for phase and energy relaxation of an oscillator coupled to a bath of particles interacting through a (spherically symmetric) Lennard-Jones potential. Although much more work is needed here the results are already very interesting. Their model reproduces the behavior in the liquid and also the jump of T_2 on solidification. In the solid the density is higher than in the liquid, but the density fluctuations are less pronounced. This forms the basic reason for the jump of T_2. No data were presented for the density dependence in the solid. To be able to compare MD results with our experiments, one needs MD simulation on more realistic systems including rotational degrees of freedom.

In this paper, we showed the feasibility of performing TSRS under high pressures. The most important problem will remain the nonresonant diamond contribution. Two approaches are proposed to reduce them; a smaller focal length or a larger gasket chamber, both of them necessary to extend measurements to higher pressures.

The class of materials suited for TSRS in a DAC is limited by the transparency of the sample. Benzene could be studied up to 5.0 GPa due to its decreasing transmission. In another experiment on CS_2 we found that it gradually decomposed due to the relative high power (20 mW average) of the incident beams, so it could only be studied in the liquid range up to 0.95 GPa. Currently, we are preparing experiments on carbon dioxide: These will not only be carried out at room temperature, but also at low temperatures (4.2 K).

ACKNOWLEDGMENTS

[1] A. Jayaraman, Rev. Mod. Phys. **55**, 65 (1983).
[2] A. Laubereau and W. Kaiser, Rev. Mod. Phys. **50**, 607 (1978).
[3] M. v. Exter and A. Lagendijk, Opt. Commun. **56**, 191 (1985).
[4] M. M. Thiery, K. Kobashi, and I. L. Spain, Solid State Commun. **54**, 95 (1985).
[5] W. D. Ellenson and M. Nicol, J. Chem. Phys. **61**, 1380 (1974).
[6] D. A. Adams and R. Applebye, Proc. R. London Soc. Ser. A **296**, 1896 (1977).
[7] J. E. Griffiths, M. Clerc, and P. M. Rentzepis, J. Chem. Phys. **60**, 3824 (1974).
[8] K. Tanabe and J. Jonas, J. Chem. Phys. **67**, 4222 (1977).
[9] S. F. Fisher and A. Laubereau, Chem. Phys. Lett. **35**, 6 (1975).
[10] J. C. H. Campbell, Ph.D. thesis, University of Illinois, 1975.
[11] T. J. Trout, S. Velsko, R. Bozio, P. L. Decola, and R. M. Hochstrasser, J. Chem. Phys. **81**, 4746 (1984).
[12] F. Ho, W. S. Tsay, J. Trout, and R. M. Hochstrasser, Chem. Phys. Lett. **83**, 5 (1981).
[13] J. P. Heritage, Appl. Phys. Lett. **34**, 470 (1979).
[14] M. v. Exter and A. Lagendijk, Rev. Sci. Instrum. **57**, 390 (1986).
[15] I. F. Silvera and R. J. Wijngaarden, Rev. Sci. Instrum. **56**, 121 (1985).
[16] P. W. Bridgman, Phys. Rev. **3**, 153 (1914).
[17] P. Figuiere, A. H. Fuchs, M. Ghelfhenstein, and H. Szwarc, J. Phys. Chem. Solids **39**, 19 (1978).
[18] S. K. Sharma, H. K. Mao, and P. M. Bell, Carnegie Institution of Washington Yearbook **79**, 359 (1980).
[19] J. Chesnoy and J. J. Weis, J. Chem. Phys. **84**, 5378 (1986).